Available online at www.sciencedirect.com
ScienceDirect
Ceramics International 37 (2011) 995–1002
CERAMICS INTERNATIONAL
www.elsevier.com/locate/ceramint

Synthesis of nanocrystalline Mn–Zn ferrite powders through thermolysis of mixed oxalates

Andre Angermann, Jörg Töpfer *

University of Applied Sciences, Dept. SciTec, Carl-Zeiss-Promenade 2, 07745 Jena, Germany

Received 2 June 2010; received in revised form 12 August 2010; accepted 6 November 2010
Available online 2 December 2010

Abstract

Nanocrystalline Mn–Zn ferrite powders were synthesized by thermal decomposition of an oxalate precursor. Two polymorphs of a mixed Mn–Zn–Fe oxalate dihydrate were obtained by precipitation of metal ions with oxalic acid: monoclinic α-$(Mn, Zn, Fe)_3(C_2O_4)_3{\cdot}6H_2O$ is obtained after precipitation and ageing at 90 °C, whereas the orthorhombic β-type is formed after precipitation at room temperature. The morphology of the oxalate crystals can be controlled by the precipitation conditions. The α-polymorph of the mixed oxalate consists of prismatic and agglomerated particles. The β-oxalate forms non-agglomerated crystallites of submicron size. Thermal decomposition of the oxalate at 350 °C in air results in an amorphous product. Nanosize Mn–Zn ferrite powders are formed at 500 °C and a mixture of haematite and spinel is observed at 750 °C. The thermal decomposition of the mixed oxalate is monitored by thermal analysis, XRD and IR-spectroscopy. The morphology of the oxalate particles is preserved during thermal decomposition; the oxide particle aggregates display similar size and shape as the oxalates. The primary particles are much smaller; their size increases from 3 nm to 50 nm after decomposition of the oxalates at 350 and 500 °C, respectively. The powder synthesized by decomposition at 500 °C was sintered at 1150 °C to dense and fine-grained Mn–Zn ferrites.

Keywords: D. Ferrites; Oxalates; Powder morphology; Nanocrystalline powders

1. Introduction

Mn–Zn ferrites represent the most important group of soft ferrites which are used for power supplies, inductors, chokes, etc. [1]. The standard processing route for commercial ferrite fabrication relies on the mixed-oxide route. However, due to the growing demand for high-quality ferrites with fine-grained, dense and homogeneous microstructures including optimum distribution of additives within the ceramics, alternative synthesis routes for sub-micron ferrite powders have been explored, e.g. hydrothermal synthesis [2], mechano-chemistry [3], sol–gel [4], micro-emulsion technique [5] and thermal decomposition of precursors [6]. The thermal decomposition of oxalate mixed crystals, as an example of the latter group of powder synthesis techniques, has already successfully been applied for the synthesis of sub-micron or nanosize powders, e.g. for Ni–Mn spinels as NTC thermistors [7] or for $BaTiO_3$ via the Ba-titanyl-oxalat route [8]. A considerable number of studies were also focused on the ferrite powder synthesis via an oxalate-based process [9–13]. Only few studies were devoted to the preparation of Mn–Zn ferrites. Bremer et al. [14], for example, reported on the synthesis and thermal decomposition of mixed (Mn, Zn, Fe)-oxalates. However, many aspects of the synthesis, crystal structures and morphology of mixed (Mn, Zn, Fe)-oxalates and their decomposition products have not been systematically investigated yet.

Ferrous oxalate dihydrate, $Fe(C_2O_4){\cdot}2H_2O$ was shown to be identical with the mineral Humboldtine many years ago [15]. The crystal structure was investigated by Mazzi and Garavelli [16] and Carić [17]. Two polymorphs were described by Deyrieux and Peneloux [18]: α-ferrous oxalate (Humboltine) has a monoclinic unit cell, space group C2/c (no. 15), with cell parameters $a_0 = 12.05$ Å, $b_0 = 5.57$ Å, $c_0 = 9.76$ Å, $\beta = 124°18'$, and $z = 4$. The β-polymorph has an orthorhombic cell, space group Cccm (no. 66), with $a_0 = 12.26$ Å, $b_0 = 5.57$ Å, $c_0 = 15.48$ Å, and $z = 8$. The α- and β-oxalates were synthesized by precipitation from ferrous salt solutions with oxalic acid either with excess or

* Corresponding author. Tel.: +49 3641 205350; fax: +49 3641 205451.
E-mail address: joerg.toepfer@fh-jena.de (J. Töpfer).

0272-8842/$36.00
doi:10.1016/j.ceramint.2010.11.019

stoichiometric oxalate/iron ratios, respectively [18]. It was shown recently, that the temperature of precipitation is another key parameter for the synthesis of either the α- or the β-oxalate [19]. Moreover, the morphology of the oxalate crystals can be tailored by selecting an appropriate temperature [19]. The α-polymorphs of Mn- and Zn-oxalate dihydrates were obtained after precipitation with oxalic acid in boiling metal ion solutions; however, no orthorhombic polymorphs were reported [20].

The thermal decomposition of oxalates generally proceeds between 200 and 400 °C; oxides are obtained as decomposition products in oxygen-rich atmospheres. Ferrous oxalate decomposes into haematite, α-Fe_2O_3, in air [21–23]. The situation is more complex, if the decomposition is performed in an atmosphere of inert or reducing gases or in closed containers, where gaseous decomposition products might form quite reducing conditions. Recently, Frost and Weier demonstrated that the decomposition under reducing conditions gives magnetite, Fe_3O_4, or iron, depending on the partial pressure of oxygen [22]. The thermolysis of mixed oxalates was shown to give ternary oxides, e.g. ferrites [9]. On the other hand, it is essential to synthesize oxalate mixed crystals in order to obtain the desired ternary (or multi-component) oxides as a result of thermal decomposition. As an example, it was shown that the mixed oxalate $NiMn_2(C_2O_4)_3{\cdot}6H_2O$ transforms into metastable $NiMn_2O_4$ spinel at 350 °C in air, whereas a mixture of Ni- and Mn-oxalates forms a mixture of binary oxides at the same conditions [24].

In this communication we report on the synthesis, crystal structure and morphology of Mn–Zn–Fe oxalates. The structure and morphology of the oxalate particles depend on the precipitation conditions. Thermal decomposition at 500 °C in air results in Mn–Zn ferrite powders. The morphology of the oxalate powder particles is maintained in the ferrite particles as result of thermal decomposition. The ferrite powder particles obtained at 500 °C display a crystallite size of 45–50 nm and are well suited for the fabrication of Mn–Zn ferrite cores.

2. Experimental

2.1. Sample preparation

Mn–Zn–Fe oxalate hydrate crystals of composition $Mn_{0.686}Zn_{0.233}Fe_{2.081}(C_2O_4)_3{\cdot}6H_2O$ were prepared by precipitation from aqueous solutions. Iron powder as starting material was dissolved in an acetic acid solution under argon. Next, Mn- and Zn-acetate hydrates (Mn- and Zn-contents determined gravimetrically) were dissolved. Subsequently, the solution of metal ions was combined under stirring with an oxalic acid solution in a three-necked flask under argon atmosphere in order to avoid oxidation of Fe^{2+}. The precipitation and ageing in argon atmosphere was performed at (i) 1 h at 20 °C (oxa04), (ii) 1 h at 90 °C (oxa05), and (iii) 7 h at 90 °C (oxa11). Finally, the mixed oxalates suspension was dried at 60 °C in a vacuum rotary evaporator in air.

The mixed (Mn, Zn, Fe)-oxalate was calcined for 2 h at 350, 500 and 750 °C, respectively, in air in a muffle furnace (Nabertherm) in flat Pt crucibles without lids. Sintered Mn–Zn ferrite cores were prepared from ferrite powders obtained by oxalate decomposition at 500 °C in air. 0.05 wt% CaO and 0.01 wt% SiO_2 were used as standard additives; 200 ppm Nb_2O_5, 250 ppm ZrO_2, 0.3 wt% SnO_2, and 400 ppm V_2O_5 were also added. The powder mixture was wet homogenized for 6 h in a polyethylene container with zirconia media on a roller bank. After drying, the powder was compacted using polyvinylalcohol as binder to give ring cores with 26 mm outer diameter. The samples were sintered in a laboratory tubular furnace with a computer-controlled atmosphere that is provided by mixing O_2 and N_2 with mass flow controllers. The samples were heated with 1.5 K/min to 1150 °C, held there for 3 h, then cooled down with 1.5 K/min according to $\log p_{O_2} = a - b/T$ with atmosphere parameters $a = 8$ and $b = 14540$.

2.2. Characterization

The oxalate and oxide particles were investigated by scanning electron microscopy SEM (DSM 940A, Zeiss, Jena, Germany). Powder X-ray diffraction measurements (XRD) were performed with a Siemens D5000 and Cu K_α radiation (step time 8 s; step size 0.02°; 10°–130° 2θ). Lattice parameters were refined using the TOPAS R software package (Bruker AXS, Karlsruhe, Germany). The specific surface A_s of the powders was determined by nitrogen adsorption (BET, Nova 2000, Quantachrome Instruments, Boynton Beach, USA); a mean primary particle size was estimated using the relation $d_{BET} = 6/\rho A_s$ with the density ρ. The crystallite size was estimated from XRD line broadening using the Scherrer equation, $d_{XRD} = K\lambda/[(B - b)\cos\theta]$, with the wave length λ, the peak width B, the instrumental broadening b ($b = 0.08°$ for standard LaB_6), the Bragg angle θ and the shape factor $K \approx 0.89$. Thermal analysis (TG, DTA) was carried out with a SETARAM TGA92 system, the samples were heated in open Pt containers (TG + DTA sample holder: diameter 3 mm, height 6 mm) in air with a rate of 2 K/min (sample mass about 20 mg). IR spectra were recorded from 4000 to 400 cm^{-1} using a Mattson FTIR spectrometer (Genesis II); 1 mg of the powdered sample was diluted with 99 mg KBr.

3. Results and discussion

The prepared Mn–Zn–Fe oxalate hydrates are yellowish powders irrespective the precipitation temperature. X-ray diffraction studies show that orthorhombic β-oxalate is observed after precipitation at 20 and 90 °C. The XRD powder pattern of the sample obtained at 20 °C (oxa04) is shown in Fig. 1. All diffraction peaks could be indexed in the orthorhombic structure (space group Cccm) as proposed by Deyrieux and Peneloux [18]. The calculated lattice parameters are $a_0 = 12.241(9)$ Å, $b_0 = 5.567(4)$ Å, and $c_0 = 15.480(9)$ Å. Precipitation at 90 °C and ageing at that temperature for 7 h (oxa11) gives the monoclinic α-polymorph (Fig. 1) with unit cell dimensions $a_0 = 11.973(2)$ Å, $b_0 = 5.555(1)$ Å, $c_0 = 9.926(1)$ Å, and $\beta = 128°45(2)'$. The lattice parameters of both polymorphs are in good agreement with those of ferrous oxalate dihydrate

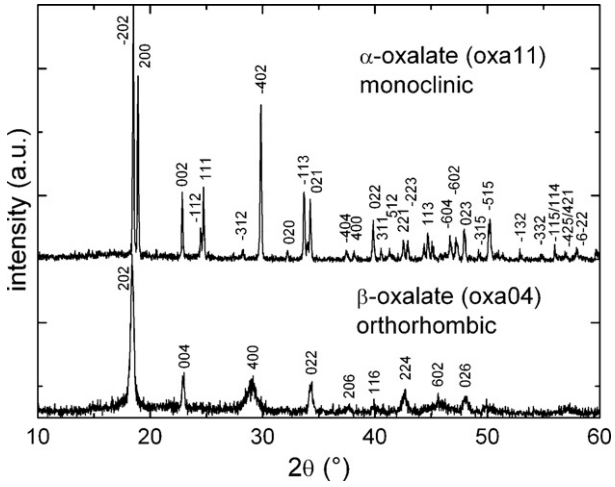

Fig. 1. XRD patterns of Mn–Zn–Fe oxalate dihydrates: β-oxalate obtained at 20 °C (lower panel) and α-oxalate obtained at 90 °C (upper panel).

[18,19]. Both polymorphs of Mn–Zn–Fe oxalate represent mixed oxalate crystals, not a mixture of the individual oxalates. This is clearly evidenced by the XRD patterns of the monoclinic α-form. However, the β-oxalate displays larger diffraction peak widths. In combination with the fact, that orthorhombic variants of Mn- and Zn-oxalate have not been reported yet, this points to a possible non-ideal mixing of the cations in the β-oxalate powder.

The α-oxalate is the thermodynamically stable modification of the mixed Mn–Zn–Fe oxalate; its formation seems to require a temperature of 90 °C for several hours for complete transformation; experiments at 90 °C with ageing periods between 1 and 7 h resulted in mixtures of α- and β-oxalates. This confirms the observations of Deyrieux et al. [20] on the metastable character of the β-oxalates of Ni, Co and Fe.

The morphologies of the Mn–Zn–Fe mixed oxalates depend on the synthesis conditions. The β-oxalate powder, precipitated at room temperature, consists of loosely agglomerated particles with particle sizes in the order of 200–1000 nm as demonstrated by SEM micrographs (Fig. 2a). Precipitation at increased

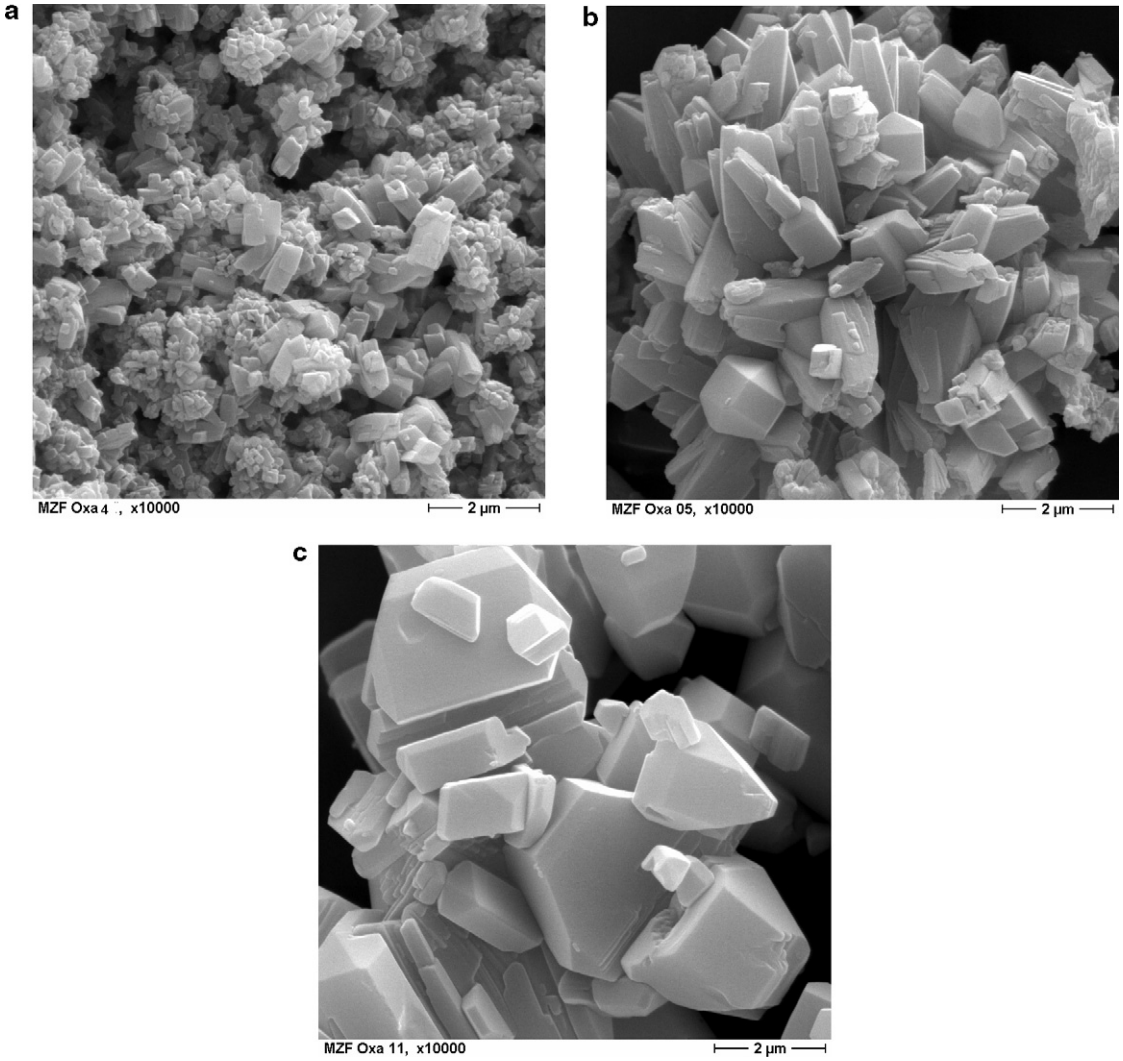

Fig. 2. SEM micrographs of Mn–Zn–Fe oxalate dihydrates prepared at 20 °C (a), 90 °C (b) and at 90 °C for 7 h (c).

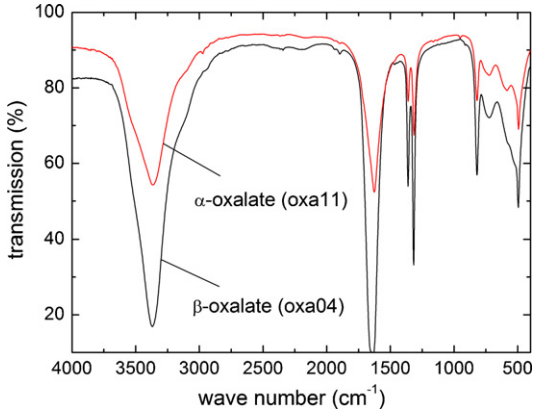

Fig. 3. Infrared spectra of α- and β-Mn–Zn–Fe oxalate dihydrates (α-oxalate prepared by precipitation/ageing at 90 °C for 7 h and β-oxalate at 20 °C for 1 h, respectively).

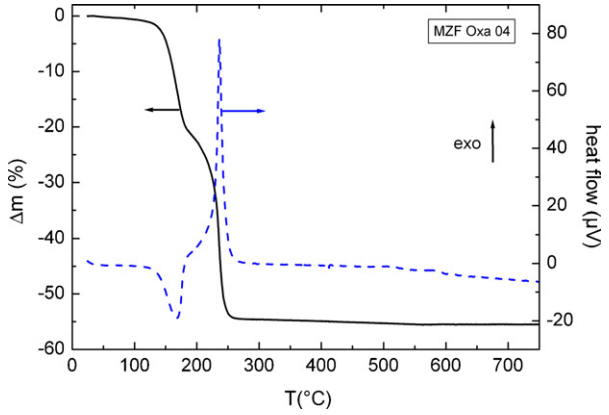

Fig. 4. Thermal analysis (TG and DTA) of β-Mn–Zn–Fe mixed oxalate in air (heating rate 2 K/min).

temperature leads to the formation of larger agglomerates; typical features are bar-shaped crystals several microns in length that form star-like aggregates (Fig. 2b). In contrast, the α-Mn–Zn–Fe oxalate powder, precipitated at 90 °C and aged for 7 h, consists of aggregated prism-shaped crystals of 1–2 μm size (Fig. 2c). This oxalate powder exhibits the typical habitus of crystals with a monoclinic unit cell.

IR spectra of the two oxalate polymorphs (Fig. 3) show the typical absorption bands of metal oxalate hydrates. A strong, broad band originating from hydrated water appears at 3300–3500 cm^{-1} (O–H stretching modes); another one at 1630 cm^{-1} is due to the H_2O bending motion [25]. Typical oxalate bands at 1630–1700 cm^{-1} originate from symmetric and antisymmetric ν(C═O) stretching modes. A double band at 1313 and 1360 cm^{-1} is due to the O–C–O stretching modes and a band at 820 cm^{-1} is characteristic of a O–C–O bending mode, respectively, [22,26,27].

The thermal decomposition of the mixed Mn–Zn–Fe oxalate hydrate in air was monitored by TG and DTA (Fig. 4a). α- and β-oxalates show identical TG and DTA curves. A mass loss sets in at 120 °C and is almost complete at 300 °C. The DTA curve exhibits an endothermic peak at 150 °C as signature of the dehydration step. A kink in the TG curve occurs at about 180 °C and at $\Delta m = 20\%$ (19.95% theoretical) which signals the end of the dehydration step. A second mass loss appears between 200 and 250 °C, which is accompanied by a sharp exothermic peak at 240 °C, corresponding to the oxalate decomposition reaction. The total mass losses are about 55% at 300 °C and 57% at 500 °C, respectively. The latter one agrees well with the calculated loss of 56.9% for the decomposition reaction:

$$Mn_{0.686}Zn_{0.233}Fe_{2.081}(C_2O_4)_3{\cdot}6H_2O + 1/2O_2 \rightarrow Mn_{0.686}Zn_{0.233}Fe_{2.081}O_4 + 3CO + 3CO_2 + 6H_2O \quad (1)$$

The fact that the mass loss at the end of the oxalate decomposition at 300 °C is slightly smaller than the expected value can be interpreted by the existence of a non-stoichiometric ferrite spinel composition. A cation-deficient spinel ferrite of this composition has all iron as ferric ions Fe^{3+}, hence, the mass loss is smaller compared to the one expected for Eq. (1). At about 500 °C this cation-deficient spinel is transformed into the stoichiometric ferrite with 0.081 Fe^{2+} per formula unit. At this temperature the mass loss expected according to Eq. (1) is reached. A small exothermic signal at 600 °C might indicate a phase transition from the single-phase spinel ferrite, formed at low temperature as a result of oxalate decomposition, into a two-phase mixture of haematite and a Fe-poor spinel.

The chemical composition of the ferrite powders obtained through thermolysis of the oxalates at 500 °C was analyzed by spectroscopy (ICP-AES). The results (Table 1) confirm that concentrations of the main components very well match the expected values and hence the ferrite powders indeed have the nominal compositions. Moreover, the concentrations of silica and calcium oxide are very low. This is of special importance, since SiO_2 and CaO are the main additives for tailoring of the sintering and grain growth behavior of Mn–Zn ferrites.

Table 1
Results of chemical analysis (measured with ICP-AES) of ferrite powders prepared by thermal decomposition of α- and β-Mn–Zn–Fe mixed oxalates at 500 °C; concentrations of main constituents (mol%) and of calcia and silica impurities (wt%).

	Main constituents (mol%)			Impurities (wt%)	
	ZnO	Fe_2O_3	MnO	CaO	SiO_2
Theoretical	11.9	53.1	35.0	–	–
β-Oxalate 500 °C	11.912 ± 0.002	53.079 ± 0.001	34.993 ± 0.003	<0.004	<0.005
α-Oxalate 500 °C	11.823 ± 0.003	53.152 ± 0.002	35.025 ± 0.003	<0.005	<0.006

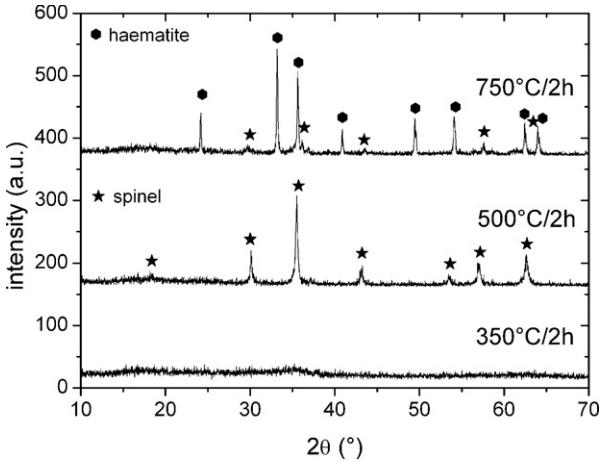

Fig. 5. XRD patterns of Mn–Zn–Fe mixed oxalates calcined at different temperatures in air.

The products of thermal decomposition of the Mn–Zn–Fe oxalate at 350, 500 and 750 °C in air were studied by XRD (Fig. 5). The powder obtained at 350 °C is amorphous. Thermal decomposition of the oxalates at 500 °C (holding time 2 h) results in the formation of a single-phase Mn–Zn ferrite. The lattice parameter of the cubic ferrite spinel is 8.495(3) Å. Decomposition at 750 °C results in a mixture of haematite (α-Fe_2O_3) and Fe-poor spinel. This is the expected phase composition in the Mn–Zn–Fe–O system at temperature of $T < 1200$ °C in air. Mn–Zn ferrites are stable at about $T > 1200$ °C only and decompose during cooling in air [28,29]. In this context, it is surprising that a single-phase spinel ferrite was formed through oxalate decomposition at 500 °C for 2 h. However, prolonged annealing at 500 °C of the ferrite powder (obtained by oxalate decomposition at 500 °C for 2 h) reveals the metastable character of that spinel phase: after annealing at 500 °C for 24 h the thermodynamically stable mixture of haematite/spinel is indeed observed (Fig. 6).

The oxide powders obtained through thermal decomposition of Mn–Zn–Fe oxalate were also investigated by IR spectroscopy. The spectrum of the sample prepared at 350 °C in air shows a broad band at 3500 cm^{-1} (not shown here) indicating a

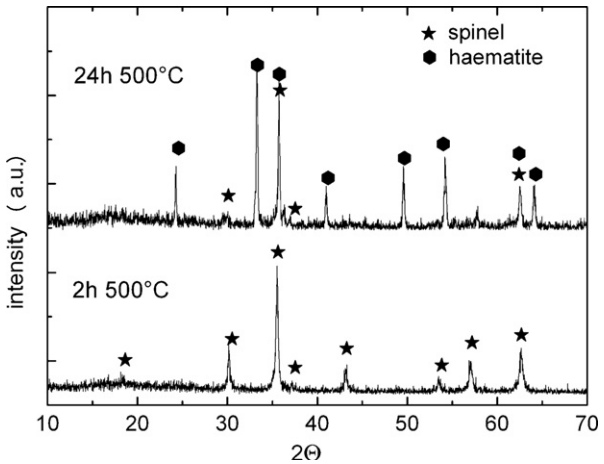

Fig. 6. XRD patterns of Mn–Zn–Fe mixed oxalates calcined at 500 °C for 2 and 24 h in air.

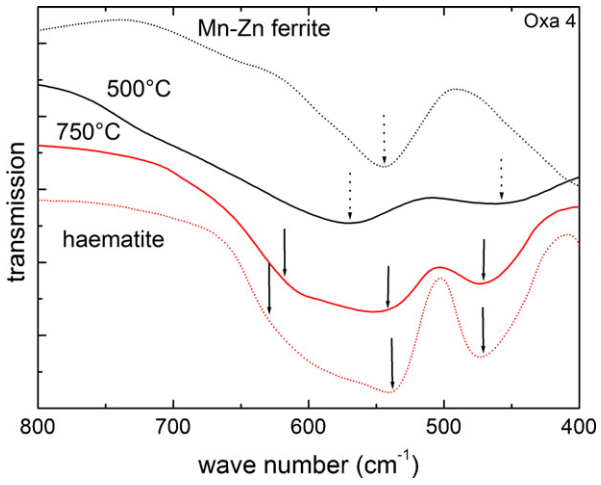

Fig. 7. Infrared spectra of oxides prepared by thermal decomposition of β-Mn–Zn–Fe oxalate dihydrate at 500 and 750 °C in air (sintered Mn–Zn ferrite and haematite for comparison).

significant concentration of adsorbed water. This is consistent with the large specific surface. Between 400 and 800 cm^{-1} the oxide powders exhibit the typical metal–oxygen bands (Fig. 7). A factor group analysis, reported in a classic IR work on spinels, resulted in four IR active bands; in most cases including ferrites only two of them are observed between 300 and 800 cm^{-1} [30–32]. For comparison Fig. 7 shows a spectrum of a sintered Mn–Zn ferrite of the same composition; one strong band at 545 cm^{-1} is found. The second band is not observed; obviously its center is located at wavenumbers $\leq$400 cm^{-1}. The IR spectrum of the sample obtained by oxalate decomposition at 500 °C for 2 h is also typical of a spinel-type oxide. However, for this ferrite one absorption band is centered at 570 cm^{-1} and the second one appears at 460 cm^{-1}. This might indicate a different cation arrangement in the low temperature metastable spinel compared to the sintered spinel ferrite; possibly the cation distribution in this spinel is highly disordered. The sample prepared at 750 °C shows several distinct bands that allow unequivocal identification of haematite (the spectrum of pure haematite is also shown in Fig. 7). Strong bands at 470 and 540 cm^{-1} and a shoulder at 630 cm^{-1} are in good agreement with IR spectra of α-Fe_2O_3 from the literature [33–35]. These findings confirm the results of the XRD study.

The morphological properties of the oxide powders were also studied (Table 2). The amorphous product obtained at

Table 2
Properties of oxide powders obtained by thermal decomposition of β-Mn–Zn–Fe oxalates at 350, 500, and 750 °C in air (specific surface area A_S, mean primary particle size from specific surface d_{BET}; crystallite size d_{XRD}; lattice parameter a_0).

T (°C)	A_S (m^2/g)	d_{BET} (nm)	d_{XRD} (nm)	Phases (XRD)	a_0 (Å)
350 °C/2 h	420	3	–	Amorphous	–
500 °C/2 h	40	50	45 ± 4	Spinel	8.495(3)
750 °C/2 h	2	570	–	Haematite & spinel	–

350 °C exhibits a large specific surface that corresponds to a particle size of about d_{BET} = 3 nm. The ferrite powder obtained after calcinations at 500 °C for 2 h has larger particles with a d_{BET} = 50 nm. From the XRD peak broadening a crystallite sizes of d_{XRD} = 45 nm was estimated. This demonstrates that the oxalate decomposition at 500 °C in air yields a nanocrystalline Mn–Zn ferrite powder. As expected, the particle size increases to sub-micron size after oxalate decomposition at

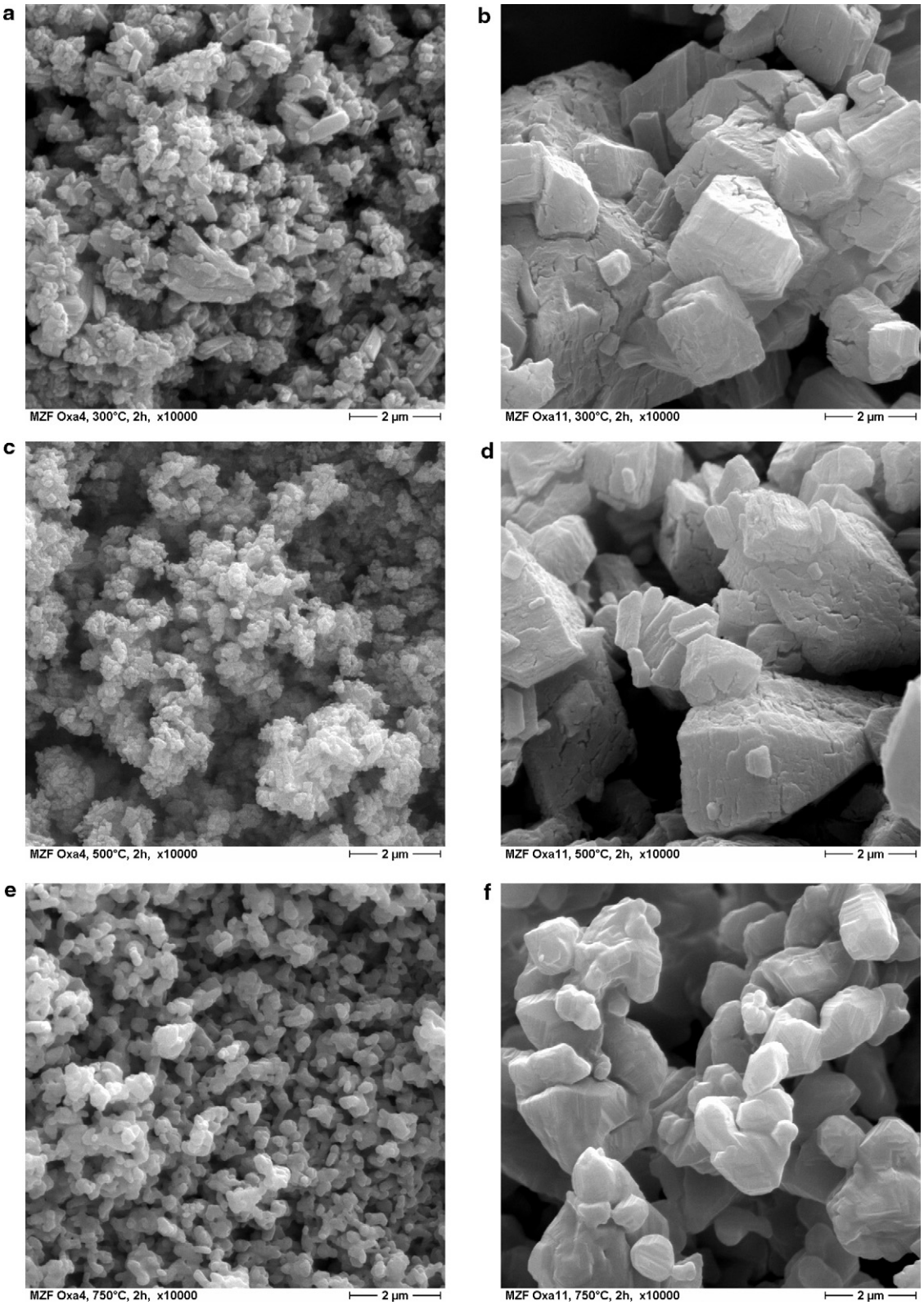

Fig. 8. SEM micrographs of oxide powders prepared by thermal decomposition of α- and β-Mn–Zn–Fe mixed oxalates, respectively: from β-oxalate at 350 °C (a), 500 °C (c) and 750 °C (e) and from α-oxalate at 350 °C (b), 500 °C (d) and 750 °C (f).

750 °C. Since the decomposition of the α- and β-oxalate lead to comparable values of the specific surface and crystallite size, we only report data from the calcinations of β-Mn–Zn–Fe oxalate in Table 2.

SEM micrographs of the oxide powders (Fig. 8) demonstrate that the morphology of the oxalate powders is preserved during thermal decomposition. The aggregate size and the shape of the oxide particles are predetermined by the oxalate morphology. The morphology of the oxide powders obtained by thermolysis of β-oxalate crystals (precipitated at 20 °C) will be discussed first. The oxide synthesized at 350 °C (Fig. 8a) exhibits an aggregate size similar to the crystal size of the β-oxalate (Fig. 2a). However, the individual primary particles or crystallites that have formed as a result of oxalate decomposition are much smaller (Table 2). Increase of the decomposition temperature to 500 °C (Fig. 8c) gives a ferrite powder consisting of loose aggregates of 1–2 μm size. The powder prepared at 750 °C (Fig. 8e) still consists of loose aggregates; grain growth (see Table 1) and the beginning of sintering and formation of sintering necks between some particles can be observed. In all three powders, the formation of soft agglomerates is observed. In contrast, thermal decomposition of the larger prism-shaped α-Mn–Zn–Fe oxalate crystals (precipitated at 90 °C, Fig. 2c) results in oxide particles with completely different morphologies. The oxide powder prepared from α-oxalate at 350 °C contains many hard aggregates of 1–3 μm size (Fig. 8b). The aggregates also form hard agglomerates of several microns in size. Comparison with the SEM micrograph of the α-oxalate (Fig. 2c) demonstrates that the morphology of the oxalate crystals is similar to those of the oxide aggregates. The ferrite powder prepared from the α-oxalate at 500 °C also consists of large and hard agglomerates of strongly connected aggregates and individual ferrite particles (Fig. 8d). The aggregates are composed of nanocrystalline particles. The sizes of the primary ferrite particles prepared from α- and β-oxalates, however, are similar, e.g. for ferrite powders synthesized at 500 °C the particle size is about 50 nm (Table 2). Calcination at 750 °C has led to hard aggregates also, with primary particles of about 0.5 μm (Fig. 8f).

The ferrite powder prepared by thermal decomposition of β-Mn–Zn–Fe oxalate at 500 °C for 2 h in air was used for preliminary sintering studies. Since this powder consists of loose aggregates with an individual primary particle size of about 50 nm, it is anticipated that this powder is well suited for the preparation of Mn–Zn ferrites with fine-grained and homogeneous microstructures. The nanosize primary particles formed as a result of low-temperature oxalate decomposition may exhibit enhanced sintering activity. On the other hand, the agglomeration behavior of the nanocrystalline powder might be advantageous for the granulation and compaction process; it is expected that the agglomerates and aggregates are easily destroyed as a result of consolidation. The powder was uniaxially pressed to a green density of 2.5 g/cm^3. Sintering was performed at 1150 °C. XRD experiments confirmed the formation of single-phase Mn–Zn ferrite with a unit cell parameter of a_0 = 8.498(1) Å. Very dense ferrite ceramics with 5.0(1) g/cm^3 (99%) were obtained. The microstructures of the ferrites consist of grains with a mean grain size of 5.8(1) μm (Fig. 9). These results show that the nanosize Mn–Zn ferrite powders are promising materials for the synthesis of low-loss power ferrites; sintering at comparably low temperatures enables the preparation of dense ferrites with small grain sizes. The effects of the variation of sintering conditions and additive concentrations on the power losses of these Mn–Zn ferrites will be reported in a next publication.

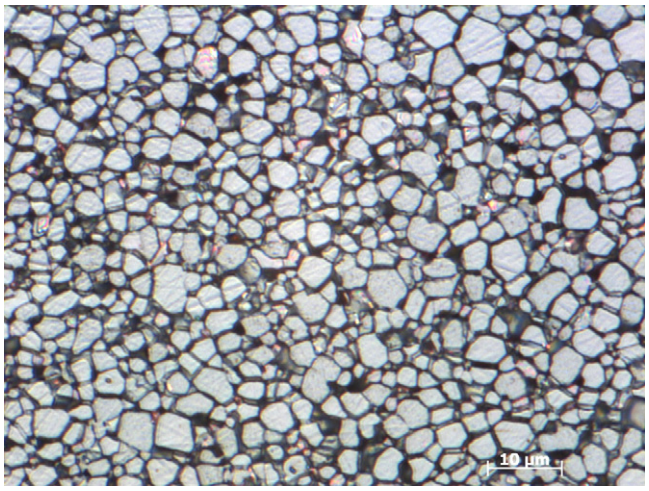

Fig. 9. SEM micrograph of a Mn–Zn ferrite prepared via the oxalate route and sintered at 1150 °C.

4. Conclusions

Mn–Zn–Fe oxalate hydrate particles were synthesized by precipitation reactions. It was shown for the first time that two polymorphs of these mixed oxalates occur. Precipitation at 20 °C results in the formation of β-oxalate with orthorhombic structure. If the precipitation is performed at 90 °C for 7 h, monoclinic α-oxalate is obtained. The morphology of the oxalates depends on the temperature of precipitation, and ranges from small, rounded and hardly agglomerated particles of β-oxalate to heavily agglomerated α-oxalate powders. Thermal decomposition of the oxalates at 500 °C in air gives a nanosize spinel ferrite powders with a large specific surface and a crystallite size of 45 nm. The morphologies of the ferrite particles resemble those of the oxalate crystals; ferrite powders of loosely or heavily aggregated crystallites are observed after decomposition of β- and α-oxalates, respectively. The nanosize ferrites are sinter-active powders that can be sintered to dense Mn–Zn ferrites with grain sizes of about 5 μm at 1150 °C.

Acknowledgements

The authors thank Mrs. M. Friedrich for SEM investigations, Mrs. K. Franke for IR and Mr. E. Hartmann for XRD measurements (all FH Jena). Financial support from the Bundesministerium für Bildung und Forschung (Germany) under the grant Fanimat Nano (03WKF22E) is acknowledged.

References

[1] M. Sugimoto, The past, presence, and future of ferrites, J. Am. Ceram. Soc. 82 (1999) 269–280.

[2] M. Rozman, M. Drofenik, Hydrothermal synthesis of manganese zinc ferrites, J. Am. Ceram. Soc. 78 (1995) 2449–2455.

[3] D. Arcos, R. Valenzuela, M. Vasques, M. Vallet-Regi, Chemical homogeneity of nanocrystalline Zn–Mn spinel ferrites obtained by high-energy ball milling, J. Solid State Chem. 141 (1998) 10–16.

[4] J. Fan, F.R. Sale, Analysis of power loss on Mn–Zn ferrite prepared by different processing routes, IEEE Trans. Magn. 32 (1996) 4854–4856.

[5] D. Yener, H. Giesche, Synthesis of pure and manganese-, nickel-, and zinc-doped ferrite particles in water-in-oil microemulsions, J. Am. Ceram. Soc. 84 (2001) 1987–1995.

[6] P. Sainamthip, V.R.W. Amarokoon, Preparation of manganese zinc ferrite powders by alcoholic dehydration of citrate/formate solution, J. Am. Ceram. Soc. 71 (1988) C92–95.

[7] A. Feltz, J. Töpfer, F. Schirrmeister, Conductivity data and preparation routes of $NiMn_2O_4$ thermistor ceramics, J. Eur. Ceram. Soc. 9 (1992) 187–191.

[8] C. Pithan, D. Hennings, R. Waser, Progress in the synthesis of nanocrystalline $BaTiO_3$ powders for MLCC, Intl. J. Appl. Ceram. Technol. 2 (2005) 1–14.

[9] D.G. Wickham, Metal iron(III) oxides, Inorg. Synth. 9 (1967) 152–156.

[10] S. Guillemet-Fritsch, S. Viguie, A. Rousset, Structure of highly divided nonstoichiometric iron manganese oxide powders $Fe_{3-x}Mn_x\square_{3\delta/4}O_{4+\delta}$, J. Solid State Chem. 146 (1999) 245–252.

[11] G.B. McGarvey, D.G. Owen, Control of the morphology and surface properties of nickel ferrite, J. Mater. Sci. 33 (1998) 35–40.

[12] H. Langbein, S. Fischer, Investigation of the formation of nickel zinc ferrite from coprecipitated oxalates, Thermochim. Acta 182 (1991) 39–46.

[13] S.A. Godake, U.R. Godake, S.R. Savant, S.S. Suryavanshi, P.P. Bakare, Magnetic properties of NiCuZn ferrites synthesized by oxalate precursor method, J. Magn. Magn. Mater. 305 (2006) 110–119.

[14] M. Bremer, S. Fischer, H. Langbein, W. Töpelmann, H. Scheler, Investigation on the formation of manganese zinc ferrites by thermal decomposition of solid solution oxalates, Thermochim. Acta 209 (1992) 323–330.

[15] E. Manasse, Oxalie (humboldtine) from cape d'acro (Elba), Rend. Acc. Naz. Lincei 19 (1911) 138–145.

[16] F. Mazzi, C. Garavelli, Structure of oxalate, $FeC_2O_4{\cdot}2H_2O$, Periodico di Mineralogia 26 (1957) 269–303.

[17] S. Carić, Amelioration de la structure de la humboldtine $FeC_2O_4{\cdot}2H_2O$, Bull. Soc. Franc. Miner. Crist. 82 (1959) 50–56.

[18] R. Deyrieux, A. Peneloux, Structure crystalline des deux forms allotropiques de l'oxalate ferreux dehydrate, Bull. Soc. Chim. France 8 (1969) 2675–2681.

[19] A. Angermann, J. Töpfer, Synthesis of magnetite nanoparticles by thermal decomposition of ferrous oxalate dihydrate, J. Mater. Sci. 43 (2008) 5123–5130.

[20] R. Deyrieux, C. Berro, A. Peneloux, Structure crystalline des oxalates dehydrates de manganese, de cobalt, de nickel et de zinc, Bull. Soc. Chim. France 1 (1973) 25–34.

[21] R. Glenn Rupard, P.K. Gallagher, The thermal decomposition of coprecipitates and physical mixtures of magnesium-iron oxalates, Thermochim. Acta 272 (1996) 11–26.

[22] R.L. Frost, M.L. Weier, Thermal decomposition of humboldtine, J. Therm. Anal. Calorim. 75 (2004) 277–291.

[23] M. Hermanek, R. Zboril, I. Medrik, J. Pechousek, C. Gregor, Catalytic efficiency of iron-(III) oxides in decomposition of hydrogen peroxide: competition between the surface area and crystallinity of nanoparticles, J. Am. Chem. Soc. 129 (2007) 10929–10936.

[24] J. Töpfer, J. Jung, Thermal decomposition of mixed crystals $Ni_xMn_{3-x}(C_2O_4)_3{\cdot}6H_2O$, Thermochim. Acta 202 (1992) 281–289.

[25] G. Rossman, Vibrational spectroscopy of hydrous components, in: F.C. Hawthorne (Ed.), Rev. Mineralogy, Vol 18: Spectroscopic methods in mineralogy and geology, 1988, pp. 193–204, Chelsea MI.

[26] M.A. Gabal, S.S. Ata-Allah, Concerning the cation distribution in $MnFe_2O_4$ synthesized through the thermal decomposition of oxalates, J. Phys. Chem. Solids 65 (2004) 995–1003.

[27] S.J. Hug, D. Bahnemann, Infrared spectra of oxalate, malonate and succinate adsorbed on aqueous surface of rutile, anantase amd lepidocroite measured with in situ ATR–FTIR, J. Electron. Spectrosc. Relat. Phenom. 150 (2006) 208–219.

[28] R. Morineau, M. Paulus, Chart of p_{O_2} vs. temperature and oxidation degree for Mn–Zn ferrites in the composition range $50 < Fe_2O_3 < 54$; $20 < MnO < 35$; $11 < ZnO < 30$ mole%, IEEE Trans. Magn. 11 (1975) 1312–1314.

[29] J. Töpfer, R. Dieckmann, Point defects and deviation from stoichiometry in $(Zn_{x-y/4}Mn_{1-x-3y/4}Fe_{2+y})_{1-\delta/3}O_4$, J. Eur. Ceram. Soc. 24 (2004) 603–612.

[30] W.B. White, B.A. DeAngelis, Interpretation of vibrational spectra of spinels, Spectrochim. Acta 23A (1967) 985–995.

[31] R.-D. Waldron, Infrared spectra of ferrites, Phys. Rev. 99 (1955) 1727–1735.

[32] B. Gillot, Infrared spectrometric investigation of submicron metastable cation-deficient spinels in relation to order–disorder phenomena and phase transition, Vib. Spectrosc. 6 (1994) 127–148.

[33] C.J. Serna, J.L. Randon, J.E. Iglesias, Infrared surface modes in corundum-type microcrystalline oxides, Spectrochim. Acta 38A (1982) 797–802.

[34] G.N. Kustova, E.B. Burgina, V.A. Sadykov, S.G. Poryvaev, Vibrational spectroscopic investigation of the goethite thermal decomposition products, Phys. Chem. Miner. 18 (1992) 379–382.

[35] S. Musić, S. Popović, M. Ristić, Chemical and structural properties of the system Fe_2O_3–Cr_2O_3, J. Mater. Sci. 28 (1993) 632–638.